Evaluation of Episodic Suspended Sediment Transport in San Francisco Bay, California through Remote Sensing

by
John J. Oram
San Francisco Estuary Institute

Nikolay Nezlin
Southern California Coastal Water Research Project

CONTRIBUTION
NO. 670

JUNE
2012

SAN FRANCISCO ESTUARY INSTITUTE
4911 Central Avenue, Richmond, CA 94804
p: 510-746-7334 (SFEI), f: 510-746-7300,
www.sfei.org

This report should be cited as:
Oram, J.J. and Nezlin, N. (2012). Evaluation of Episodic Suspended Sediment Transport in San Francisco Bay, California through Remote Sensing. A Report of the Regional Monitoring Program for Water Quality in San Francisco Bay. Contribution No. 670. San Francisco Estuary Institute, Richmond, California.

June 2012

Evaluation of Episodic Suspended Sediment Transport in San Francisco Bay, California through Remote Sensing

John J Oram, San Francisco Estuary Institute
Nikolay Nezlin, Southern California Coastal Water Research Project

Executive Summary

Moderate resolution satellite imagery was combined with in-situ observations of suspended sediment flux from the Sacramento-San Joaquin River Delta to gain an understanding of event-scale suspended sediment budgets for San Francisco Bay. The event-scale budgets estimated were dependent on tidal conditions, duration of the high-flow event, and the timing of the remote observation during the high-flow event. The exported fraction of suspended material entering the Bay from the Delta during high-flow conditions was greatest during ebb tides. Short, storm-driven high-flow events exported a larger fraction of their suspended sediment load than did longer-duration high-flow events such as spring snowmelts. The dependence of the event-scale budgets on environmental and meteorological conditions, combined with the lack of site-specific algorithms for estimating suspended sediment concentrations from remote observations, rendered inconclusive our attempts to develop a 'rule-of-thumb' regarding the fraction of sediment influx from large storms that passes through the system. It is possible that site-specific algorithms and an increased sample size (i.e., more remote observations) combined with in-situ observations of sediment fluxes through the Golden Gate would improve the ability of the methods presented here to develop such a 'rule-of-thumb.'

Introduction

Monitoring suspended sediment concentrations (SSC) in coastal waters and estuaries is crucial for ecosystem management. Suspended sediment plays a critical role in wetland restoration, dredging, ecosystem productivity, and water quality (Schoellhamer, 2009). SSC monitoring is traditionally done in-situ, with measurements representing concentrations at a few discrete points in space and time. However, recent advances in satellite remote sensing allow for synoptic views of coastal and estuarine dynamics. Remote sensing data analyses are drastically altering perceptions of coastal ocean transport processes.

Ruhl et al. (2001) conducted a combined remote sensing and *in-situ* study of San Francisco Bay using advanced very high resolution radiometers (AVHRR, 1 km spatial resolution) aboard the NOAA polar-orbiting weather satellites and *in-situ* optical backscatter sensors. The authors identified effects of physical processes associated with freshwater flow, wind-waves, and the spring-neap tidal cycle. However, an estimate of an event-scale suspended sediment budget was not made. Additionally, the authors noted that results could be significantly improved with even higher resolution imagery.

Development of an event-scale suspended sediment budget has the potential to significantly improve current estimates of contaminant loading from the Delta to the Bay. It is known that episodic sediment (McKee et al., 2006) and contaminant loads (David et al., 2009) account for a significant portion of annual loads. However, at present we know very little about the fate of these loads both within the Bay and exiting the Golden Gate at the time scales of these episodic events. This paper utilizes moderate-resolution MODIS satellite imagery to develop an episodic suspended sediment budget for San Francisco Bay.

Data and Methods

Selection of high-flow events

The first step in developing an event-scale suspended sediment budget was to identify periods of high Delta outflow. A time series of Delta outflow from June 24, 2002 to September 30, 2006 as estimated by the Dayflow model (IEP, 2008) is shown in Figure 1. This time period is coincident with the period for which satellite observations were obtained. Analysis of these daily flow rates indicated that a threshold of 1,500 m^3/s for defining high-flow events (David et al., 2009) yielded several multi-day events each year. Using this threshold, eleven high-flow events were identified (Table 1) for further analysis.

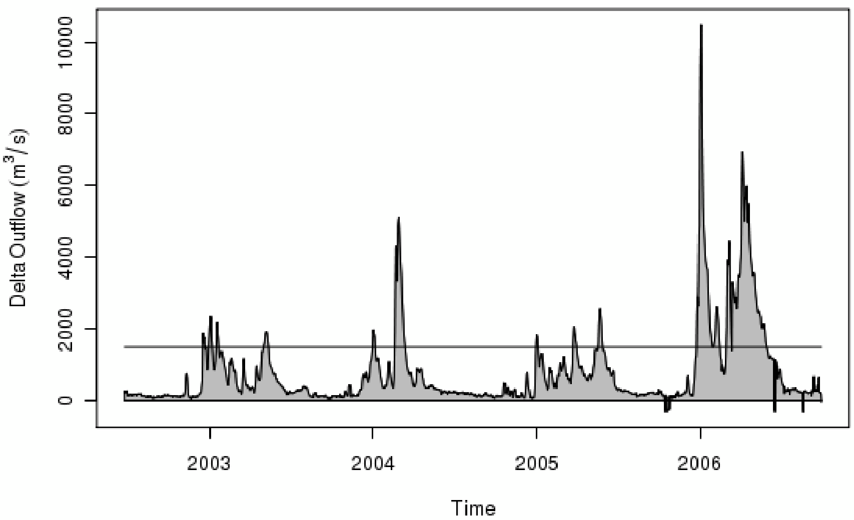

Figure 1 - Total Delta outflow as estimated by the Dayflow model (IEP, 2008). The horizontal line indicates the 1,500 m^3/s threshold used to define high-flow events.

Table 1 – High-flow events identified in the Delta outflow record shown in Figure 1.

Event #	Start High-Flow	End High-Flow	Duration (Days)	Comment
1	12/16/02	12/23/02	7	
2	12/30/02	1/5/03	6	
3	1/15/03	1/20/03	5	
4	5/1/03	5/13/03	12	
5	12/31/03	1/5/04	5	
6	2/18/04	3/12/04	23	Spring Melt
7	12/30/04	1/4/05	5	
8	3/23/05	3/31/05	8	
9	5/18/05	5/28/05	10	
10	12/25/05	2/14/06	51	Storm-driven Flood
11	2/28/06	5/29/06	90	Spring Melt

Satellite data

The satellite images used in this study were collected by Moderate-Resolution Imaging Spectroradiometer (MODIS) instruments. MODIS instruments operate onboard two near-polar sun-synchronous satellite platforms orbiting at 705 km altitude: Terra (since February 24, 2000) and Aqua (since June 24, 2002). In this study, only Aqua imagery was used. Aqua passes the equator from south to north at approximately 13:30 local time. As such, all the images used in this study were acquired within 2 hours after local noon. The MODIS sensors collect data in 36 spectral bands, from 400 to 14,000 nm.

MODIS images were collected in 2002-2006 during eleven high-flow events identified in Table 1. Any satellite observations falling within a high-flow event or within seven days after the end of the high-flow event were collected. Using a seven-day window after the end of a high-flow event improved the odds of obtaining at least one clear image related to each high-flow event. Preliminary (graphical) analysis of all MODIS images indicated that the seven-day window was sufficient for this purpose (Figure 2) while still retaining sufficient temporal proximity to be associated with a given high-flow event. Selected images were processed to obtain true-color images and remotely-sensed reflectances (Rrs).

To produce true-color images, we utilized bands 1 (250 m spatial resolution, 620-670 nm, red), 3 (500 m resolution, 459-479 nm, green), and 4 (500 m resolution, 545-565 nm, blue). The 500 m green (band 4) and blue (band 3) monochrome bands were sharpened to 250 m resolution using fine details from the higher resolution red band (band 1). Then, the contrast of each of these monochrome bands was increased to emphasize maximum details in the region of interest. Finally, all three monochrome bands (i.e., red, green, and blue) were combined to form a single true-color image. Similar methodologies were used in a study of stormwater plumes over San Pedro Shelf in southern California (Ahn et al., 2005).

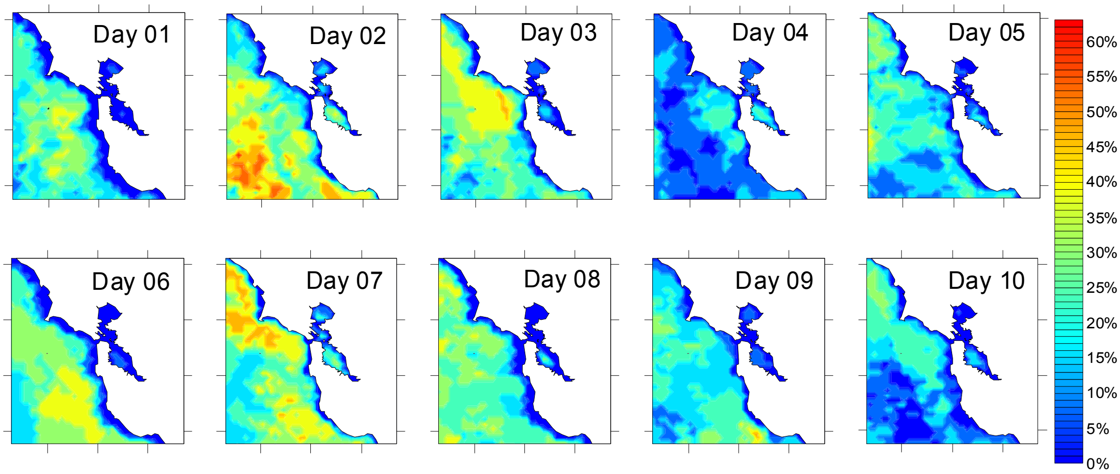

Figure 2 - Percentage of not cloud-masked Level 3 MODIS-Aqua imagery (i.e., ability to obtain clear image) during the 10 days following elevated flow (>1500 $m^3 s^{-1}$).

Remotely-sensed reflectances (Rrs) at 645 nm wavelength were calculated using the freely-available SeaDAS 5.0 software (McClain et al., 2004). The Rrs parameter was computed as Rrs = nLw(λ) / F0(λ), where nLw is normalized water-leaving radiance (i.e., the upwelling radiance just above the sea surface, in the absence of an atmosphere, and with the sun directly overhead), F0 is mean solar irradiance and λ is wavelength (Gordon and Wang, 1994). F0 for 645 nm was 158.74 mW cm^{-2} µm.

Atmospheric correction of MODIS images was achieved by the combined near-infrared/shortwave infrared (NIR-SWIR) method (Wang and Shi, 2007), which was developed especially for analysis of coastal data. The traditional method of atmospheric correction used for processing MODIS imagery is based on two NIR bands used for identifying aerosol type and correcting aerosol contributions at the visible wavelengths (Gordon and Wang, 1994; Gordon, 1997). This method works well for open ocean waters but fails in turbid coastal waters (Wang and Shi, 2005). In turbid waters two shortwave infrared (SWIR) bands are preferable for atmospheric correction, because ocean surface reflectance in SWIR is close to zero regardless of suspended matter and dissolved organic matter (i.e., CDOM) concentrations (Wang, 2007; Wang et al., 2007). However, the MODIS SWIR bands were designed for land and atmospheric applications, making them less suitable for ocean color products (Wang, 2007). Thus, the combined NIR-SWIR method for MODIS ocean color processing (Shi and Wang, 2007; Wang and Shi, 2007) was used in this study. Previous studies have illustrated that this approach results in acceptable quality ocean color products without obvious discontinuities (Wang and Shi, 2007).

Once corrected for atmospheric conditions, MODIS images were processed to estimate Total Suspended Matter (TSM, mg/L) concentrations using the empirical equation suggested by Hu et al. (2004):

$$TSM = 0.1915e^{(624.72 \times Rrs)} \quad \text{(Eq. 1)}$$

Pixels associated with atmospheric correction failure, land, cloud or ice, stray light, and sun glint were excluded from analysis.

It must be noted that the empirical relationships between Rrs and TSM are very site-specific. Previous studies revealed different empirical equations resulting in significantly different TSM estimations (Table 2). As such, we consider the TSM estimates obtained by Equation 1 as preliminary. Further research is required to develop relationships between Rrs and TSM specific to San Francisco Bay and surrounding areas.

The mass of TSM in the water column was estimated for three regions (Figure 3) assuming a homogenous vertical distribution of TSM within the top 5 m of the water column. The selection of 5 m as the depth of the plume was made by examining historic salinity data collected along the central axis of the Bay. During January of 1995 the sampling coincided with a relatively high-flow event from the Delta (peak flow = 7020 m^3/s). A cross-section of salinity measurements during this time shows that, near the Golden Gate, fresh water from the Delta is generally restricted to the upper 5 m of the water column in Central Bay, the Bay segment directly connected to the Pacific Ocean via the Golden Gate (Figure 4).

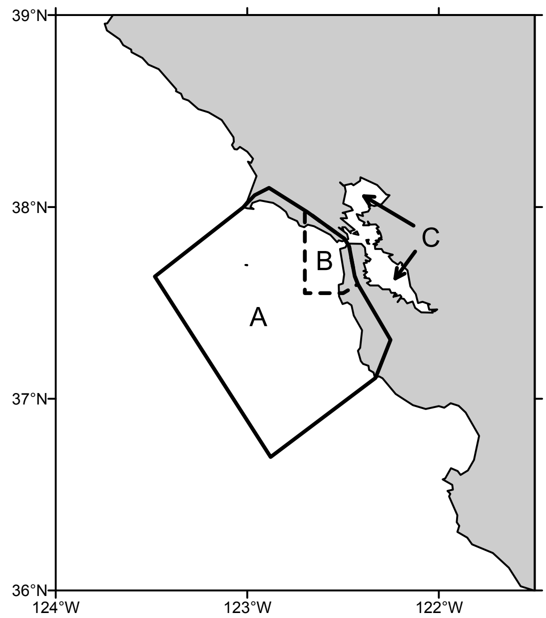

Figure 3 - The areas outside (A), near the mouth (B) and within (C) the San Francisco Bay where total TSM was calculated. Region A is inclusive of region B.

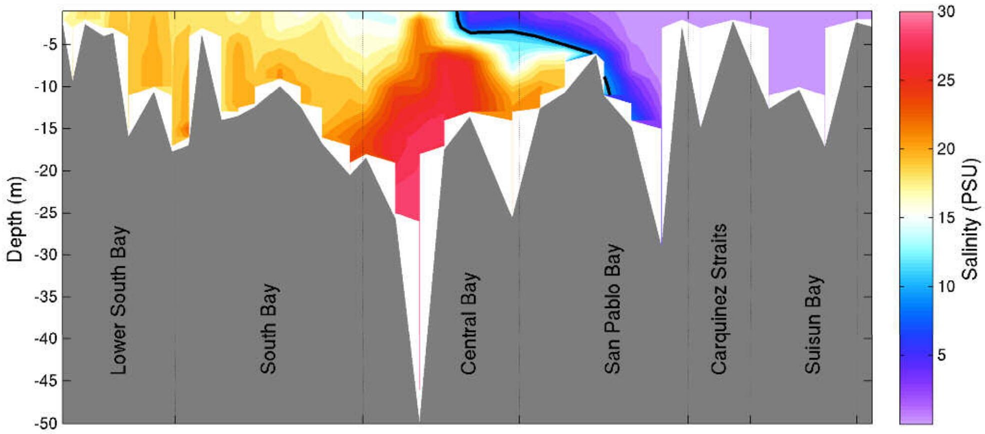

Figure 4 – Salinity cross-section of San Francisco Bay from January 15, 1995. Data were collected along the central axis of the Bay. Sampling coincided with a period of relatively high Delta outflow (peak flow was 7020 m^3/s on January 12, 1995). The black contour line indicates a salinity of 10 PSU. Data are from the USGS (http://sfbay.wr.usgs.gov/access/wqdata/).

Table 2 - The empirical relationships between Total Suspended Matter concentrations (mg/L) and Remotely-sensed Reflectances (Rrs) reported by different authors.

Equation	Author
TSM = 0.1915 x exp(624.72 x Rrs)	Hu et al. (2004)
TSM = 110.3 x Rrs + 2.0	Sipelgas et al. (2006)
TSM = -1.91 + 1140.25 x Rrs	Miller and McKee (2004)[1]

[1] In Miller and McKee (2004) the « + » (plus) was shown as a typographical error of « x » (multiplication) isntead.

Estimation of suspended sediment loads

The Central Valley of California supplies the majority (annually 94%) of fresh water to the Estuary via the Sacramento and San Joaquin River Delta and is the single largest source of suspended sediment loads. The daily mass loading of suspended sediments entering San Francisco Bay via the Delta was estimated following the methods of McKee *et. al.* (2006). Briefly, daily Delta outflow (Q, Figure 1) was combined with average daily suspended sediment concentrations (SSC, Figure 5) measured at Mallard Island (Figure 3) according to Equation 2, which accounts for landward dispersive load.

$$L_{ssc} = Q \times SSC \times \left(1 - 3.34 \times Q^{-0.398}\right) \qquad \text{(Eq. 2)}$$

Cumulative loads were generated for each high-flow event listed in Table 1. The period over which cumulative loads were estimated was extended by seven days beyond the event's end date for events where MODIS images were within this time window.

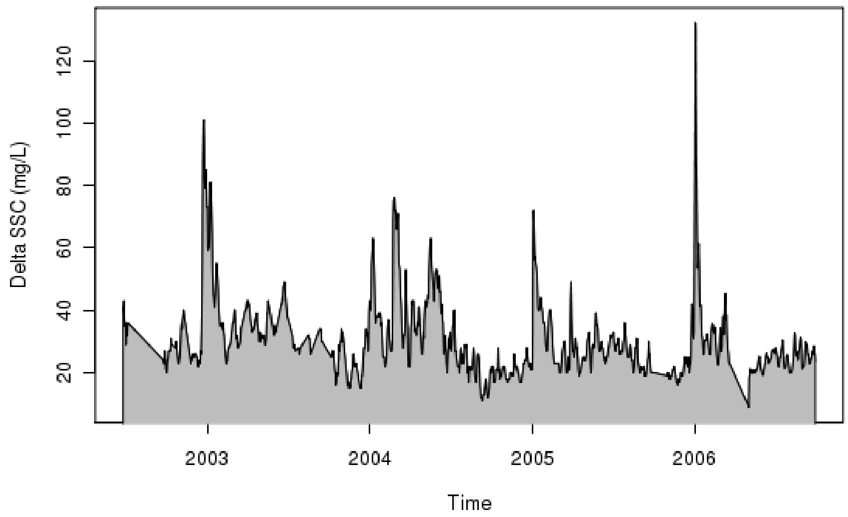

Figure 5 – Average daily suspended sediment concentration (SSC, mg/L) at Mallard Island for the time period June 24, 2002 to September 30, 2006.

Results and Discussion

A total of 20 MODIS observations made during the 11 high-flow events identified in Table 1 were selected for analysis (Table 3). The true-color images for each of these observations are included in the Appendix to this report (Figures A.1-A.20). Included with these true-color images are plots of cumulative sediment loads from the Sacramento-San Joaquin River Delta, estimated by Equation 2, for each high-flow event. No usable MODIS images were available during events 5 (12/31/03-1/5/04) and 7 (12/30/04-1/4/05).

The mass of total suspended material (TSM) estimated from satellite observations for each region, expressed as a percentage of cumulative Delta load, is summarized in Table 3. Also included are cumulative sediment loads from the Delta and Guadalupe River and tidal information for the time of the MODIS observation. Regional results were highly variable; the mass of suspended material in region A ranged from 4-1,690% of cumulative Delta loads with a median of 16%; mass estimates in region B ranged from 1-825% with a median of 4%; mass estimates in region C ranged from 2-27,300,000% with a median of 6,820%. While such variability is not unexpected (San Francisco Bay is a dynamic environment with varying tides, winds, waves, and freshwater flows) the extreme values estimated for region C are beyond any realistic expectation, even when considering inputs from local tributaries (e.g., Guadalupe River, Figure 3). These extreme values are most likely an artifact of the algorithm used to estimate TSM, which is not appropriate for the turbid, shallow waters of San Francisco Bay, where resuspension of bed sediments can contribute to the observed mass. Therefore, in the absence of a locally derived or applicable equation, region C, was excluded from further analysis.

Table 3 - Selected MODIS images by high-flow event (Table 1) including the estimated mass of suspended material in each region (expressed as a percent of cumulative Delta load), estimated cumulative loads from the Delta and Guadalupe River, and tidal information[*]. No usable MODIS images were available for events 5 and 7.

Event #	MODIS Date	Mass of TSM (million kg)			Cumulative Delta Suspended Sediment Load[2] (million kg)	Cumulative Guadalupe Suspended Sediment Load[2] (millon kg)
		Region A[1]	Region B	Region C		
1	12/18/02	165.3	80.6	11771.5	9.8	6.5
2	1/6/03	43.8	24.7	386392.5	69.6	0.3
3	1/17/03	23.0	11.2	19519.7	16.0	0.0
4	5/12/03	14.9	1.8	289.9	45.9	0.2
4	5/19/03	12.4	2.3	273.2	65.2	0.2
4	5/20/03	13.0	1.8	559.0	67.5	0.2
6	3/8/04	27.3	7.9	98370.3	329.0	1.9
6	3/10/04	29.6	10.7	161502.8	341.7	1.9
8	4/5/05	20.0	7.8	11084.5	46.3	0.2
9	5/21/05	16.7	2.9	2041.6	16.0	NA
9	6/1/05	9.0	0.6	1.5	67.1	NA
9	6/6/05	17.0	4.1	505.8	78.8	NA
10	1/9/06	817.6	766.1	153490839.8	562.0	2.1
10	1/23/06	27.7	9.3	617830.4	708.5	2.1
10	2/8/06	47.9	31.2	87147.8	771.5	2.1
11	4/17/06	35.0	11.4	312.2	346.8	9.1
11	5/1/06	37.7	10.7	648.6	401.0	9.1
11	5/8/06	22.1	5.2	9983.9	427.3	9.1
11	5/13/06	20.6	3.0	946.1	445.8	9.1
11	5/24/06	23.3	5.3	690.5	482.0	9.1

[1] Region A is inclusive of Region B

[2] Load is cumulative from event start date through date of MODIS image.

[*] Tidal information was obtained for station 9414290 (San Francisco Bay) from http://tidesandcurrents.noaa.gov.

Segregation of results for regions A and B by tidal stage provided insight on the effects of tides on transport of suspended material from the Delta through the Golden Gate. By categorizing each observation into one of four general tide classes (ebb, flood, slack high, and slack low) it became apparent that the percent of cumulative Delta loads transported beyond the Golden Gate was often greater during periods of ebb tide (Figure 6). This finding is consistent with a previous study by Ruhl *et al.* (2001) and makes conceptual sense; high freshwater discharges and ebb tides combine to increase seaward transport. The percent of cumulative Delta loads transported into regions A and B were significantly higher for ebb periods, but flood, slack high, and slack low conditions were not significantly different from one another.

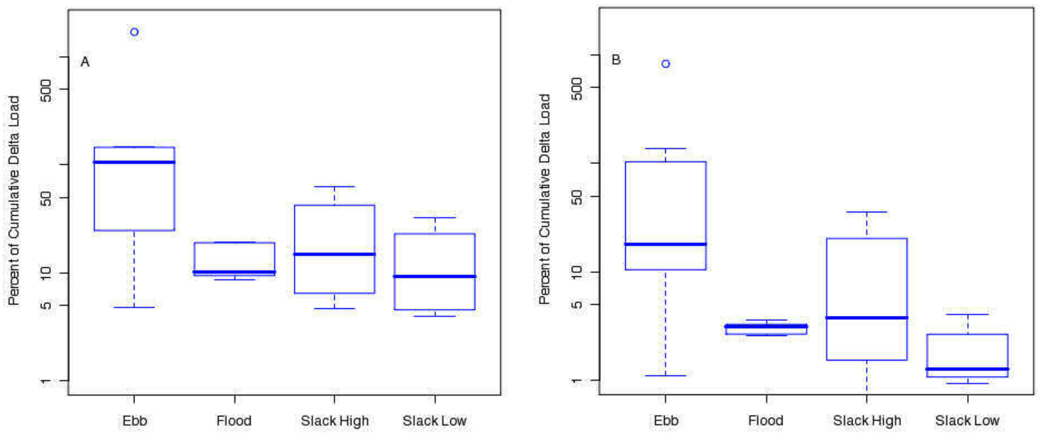

Figure 6 – Estimated percent of cumulative Delta sediment loads in regions A (left) and B (right) as a function of tidal cycle. Bold horizontal lines in each box indicate the median. The scatter points in the Ebb column indicate a statistical outlier.

Knowing which tidal phase is associated with the greatest export of material transported from the Delta during high-flow conditions is useful. Tidal phase alone, however, is not a sufficient predictor of the percent of Delta loads exported through the Golden Gate, as evidenced by the rather large range of percent of suspended sediment transported through the Golden Gate in each tidal class in Figure 6. An attempt was made to identify additional variables to improve predictive ability. Two predictive variables that make sense conceptually were identified: time since start of event and duration of event. Time since start of event indicates the timing of the satellite observation relative to the onset of the high-flow event. Event duration is a measure of the length of the high-flow event and has no dependence on the timing of the satellite observation.

Regardless of tidal phase, nearly 100% of sediment transport occurred within 20 days of the beginning of an event as shown by correlation between percent of cumulative Delta loads remaining suspended in these regions outside the Golden Gate and time since start of high-flow event (Figure 7). A locally weighted polynomial regression (LOESS) with time since start of event as the predictor was used to identify patterns within the estimates. The LOESS analysis was performed on all results for regions A and B except for event number one (12/18/02), independent of tidal stage. This event was excluded from analysis after being identified as an outlier in Figure 6. The percent of Delta loads remaining suspended in regions outside the Golden Gate during high-flow events appears to decrease as the elapsed time of the storm event increases (Figure 7). In other words, a larger percentage of Delta loads are exported at the beginning of high-flow events than is exported towards the end of high-flow events. The same finding holds true when the duration of the high-flow event is used as the predictive variable, particularly in Region A (Figure 8). This suggests that short high-flow events (e.g., rain storm-driven flows) transport a higher fraction of their total suspended material to the Pacific Ocean than do longer duration events (e.g., spring snow melts). This is consistent with other studies that relate retention of mass in estuaries to storm events (e.g., Nixon et al., 1996; McKee et al., 2000; Hossain et al., 2001; Robson et al., 2008)

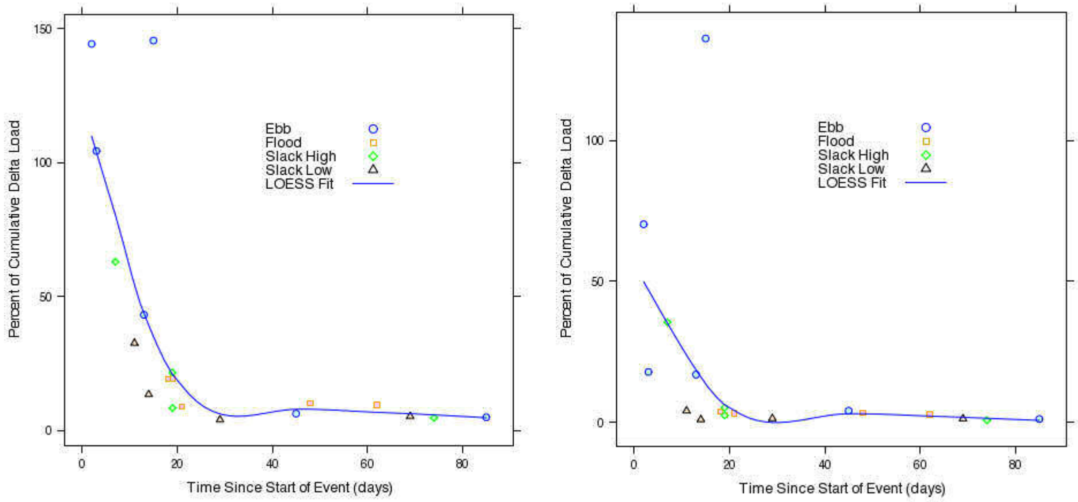

Figure 7 – Estimated percent of cumulative Delta sediment loads in regions A (left) and B (right) as a function of time since start of event. The solid line represents the results of a locally weighted polynomial regression (LOESS). High-flow event 1 was excluded from this analysis after being identified as a statistical outlier in Figure 6.

Confounding this interpretation, however, is the fact that many of the MODIS observations near the beginning of high-flow events coincided with ebb conditions, thereby introducing potential bias into the LOESS analysis in Figures 7 and 8. When the ebb tide events are excluded, this bias is less prevalent in Region A than it is in Region B (Figures 9 and 10), perhaps indicating that material that is exported further into the Pacific Ocean in Region A is less susceptible to transport back into the Bay upon reversing tides and/or waning freshwater flows.

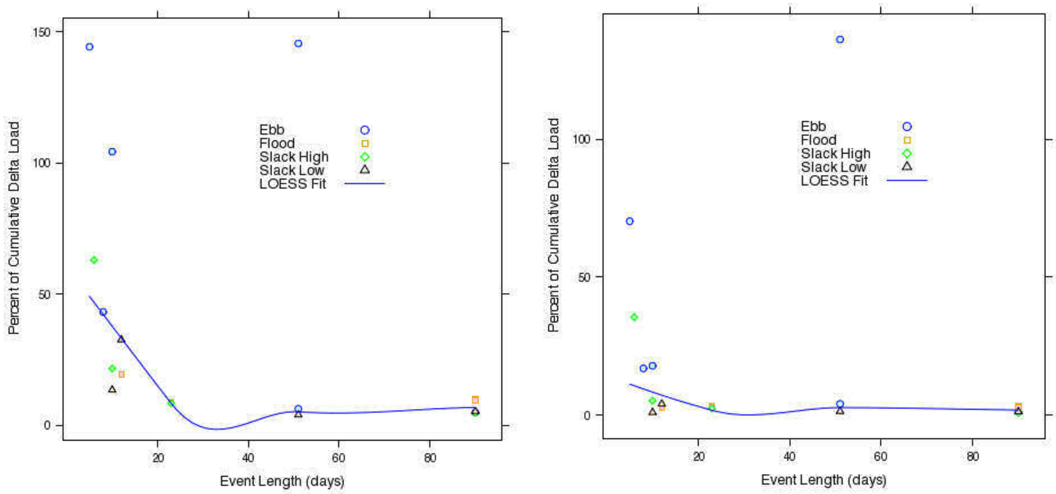

Figure 8 - Estimated percent of cumulative Delta sediment loads in regions A (left) and B (right) as a function of event length. The solid line represents the results of a locally weighted polynomial regression (LOESS). High-flow event 1 was excluded from this analysis after being identified as a statistical outlier in Figure 6.

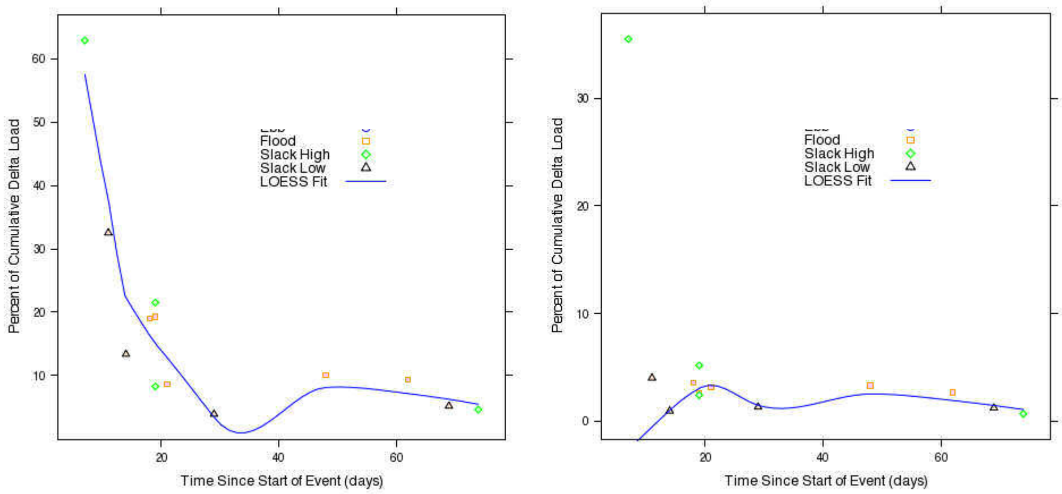

Figure 9 - Estimated percent of cumulative Delta sediment loads in regions A (left) and B (right) as a function of time since start of event, excluding high-flow events during ebb conditions. The solid line represents the results of a locally weighted polynomial regression (LOESS).

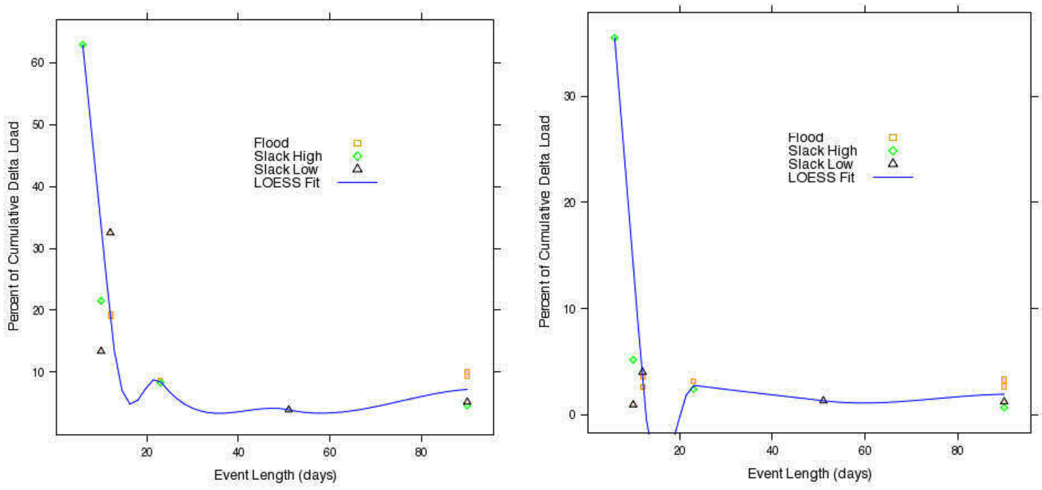

Figure 10 - Estimated percent of cumulative Delta sediment loads in regions A (left) and B (right) as a function of event length excluding high-flow events during ebb conditions. The solid line represents the results of a locally weighted polynomial regression (LOESS).

Uncertainties

A number of uncertainties surround the findings presented in this report. The most significant uncertainties are detailed here.

Satellite Algorithms

The algorithms used to process the MODIS observations are inherently uncertain. The most up-to-date algorithms, which were developed specifically for coastal and/or estuarine waters, were used in this study. Still, these algorithms are not specific to the San Francisco Bay area. Further research, including fieldwork to ground-truth estimates, is required to develop such site-specific algorithms. Such ground-truthing data is needed to estimate the uncertainty in estimates of TSM made by satellite observations.

Vertical Distribution of Suspended Material

Very little is known regarding the actual vertical distribution of TSM in the water column during high-flow events, owing in large part to the difficulty of sampling San Francisco Bay and the coastal ocean during such high-energy events. The U.S. Geological Survey, in collaboration with U.C. Berkeley and the Romberg Tiburon Center, has conducted surveys across the Golden Gate during periods of high freshwater flow (D. Hanes, St. Louis University, Personal Communication). Preliminary results were inconclusive in determining the vertical profile of TSM during such events. Different scenarios of the vertical distribution of TSM were applied when estimating the total mass of TSM in each region from satellite observations in order to gauge the uncertainty of the resulting mass estimates. These scenarios included uniform TSM with depth, increasing TSM with depth, decreasing TSM with depth, and a triangular distribution with the maximum concentration at 2.5 meters (Figure 11). In the end, these scenarios perturbed the estimated mass of TSM by a factor of 0.5–1.5.

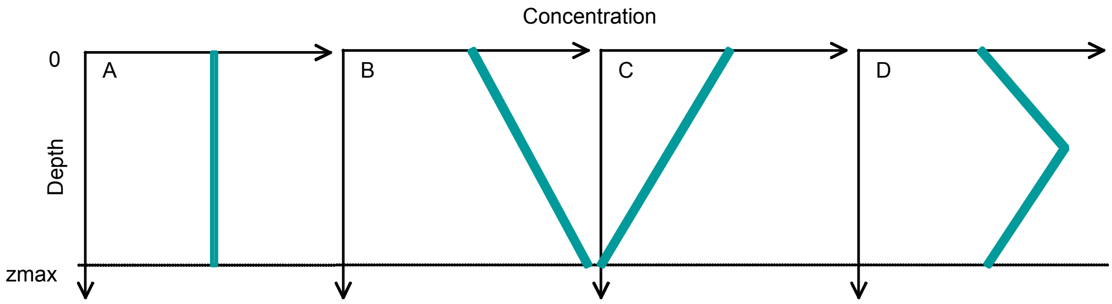

Figure 11 – Vertical distributions used to test sensitivity of TSM estimates made by remote observations. A maximum depth (zmax) of 5 meters was used for each scenario.

Fate of Material Outside Golden Gate

Knowing the ultimate fate of suspended material outside the Golden Gate is important to refining the estimates made in this pilot study. For example, understanding how much of the exported material is deposited in areas where it is susceptible to re-working by tides, winds, and waves and ultimately transport back into the Bay is likely to have significant influence on the event-scale export estimates made by this study. Ongoing studies by the U.S. Geological Survey are addressing this information gap. Of specific interest to these researchers is the transport of sand between Central San Francisco Bay and the coastal beaches adjacent to the Golden Gate*. Findings from these studies will be useful for refining the estimates of event-scale export of suspended material presented here.

Effects of Coastal Processes

Many of the MODIS images in Figures A.1-A.20 show coastal processes actively suspending material in the water column and transporting it offshore. Some of the filaments created by these coastal processes are very near, and in some cases within, the regions used for analysis of MODIS images in this pilot study (regions A and B in Figure 3). Such coastal filaments, when they exist in regions A or B, bias high the estimates of suspended material in the Bay-plume. It is difficult to quantify the degree to which such coastal processes influence the estimates made in this pilot study. Analysis of MODIS images during low freshwater flows, when a Bay-plume is absent, could help in developing a rough estimate of the 'background' contribution of coastal-derived suspended material to the mass estimates made by this study.

* See http://walrus.wr.usgs.gov/coastal_processes/sfbight/intro.html for more information on the USGS sand/sediment study.

Conclusions

The combination of moderate resolution satellite imagery with in-situ observations of suspended sediment flux at the Sacramento-San Joaquin River Delta is valuable for developing an event-scale budget of suspended material for San Francisco Bay. The event-scale budgets estimated by this pilot study were dependent on tidal conditions, duration of the high-flow event, and the timing of the remote observation during the high-flow event. The exported fraction of suspended material entering the Bay from the Delta during high-flow conditions was greatest during ebb tides. Short, storm-driven high-flow events exported a larger fraction of their suspended sediment load than did longer-duration high-flow events such as spring snowmelts.

The dependence of the event-scale budgets on environmental and meteorological conditions, combined with the lack of site-specific algorithms for estimating suspended sediment concentrations from remote observations rendered inconclusive our attempts to develop a ‘rule-of-thumb’ regarding the fraction of sediment influx from large storms that passes through the system. It is possible that site-specific algorithms and an increased sample size (i.e., more remote observations) combined with in-situ observations of sediment fluxes through the Golden Gate would improve the ability of the methods presented here to develop such a ‘rule-of-thumb’, but significant challenges remain to quantitatively measuring TSM outside the Bay during storm events. Additional challenges include the contribution of ‘background’ TSM from resuspended sediment both within the Bay and in near-shore coastal areas, which confound estimates of sediment loads entering and leaving the Bay.

An alternative approach to address this unknown is to combine the methods implemented in this study with a spatially resolved model of San Francisco Bay. In this approach event-scale budgets developed through remote observations can be used to validate event-scale budgets developed though hydrodynamic modeling. The validated model can then be used to examine the behavior of multiple events for which remote observations are not available. Analysis of a large number of events in this way would allow for a more precise estimate of the sediment influx from large storms that passes through the system.

References

Ahn, J.H., Grant, S.B., Surbeck, C.Q., DiGiacomo, P.M., Nezlin, N.P., Jiang, S., 2005. Coastal water quality impact of stormwater runoff from an urban watershed in southern California. Environmental Science & Technology 39: 5940-5953.

David, N., McKee, L.J., Black, F.J., Flegal, A.R., Conaway, C.H., Schoellhamer, D.H., Ganju, N.K., 2009. Mercury concentrations and loads in a large river system tributary to San Francisco Bay, California, USA. Environmental Toxicology and Chemistry 28, No. 10, 2091–2100.

Gordon, H.R., 1997. Atmospheric correction of ocean color imagery in the Earth Observing System era. Journal of Geophysical Research-Atmospheres 102: 17081-17106.

Gordon, H.R., Wang, M., 1994. Retrieval of water-leaving radiance and aerosol optical thickness over the oceans with SeaWiFS: a preliminary algorithm. Applied Optics 33: 443-452.

Hossain, S., Eyre, B., and McConchie, D., 2001. Suspended sediment transport dynamics in the sub-tropical micro-tidal Richmond River Estuary, Australia. Estuarine, Coastal and Shelf Science 52, 529-541.

Hu, C., Chen, Z., Clayton, T.D., Swarzenski, P., Brock, J.C., Muller-Karger, F.E., 2004. Assessment of estuarine water-quality indicators using MODIS medium-resolution bands: initial results from Tampa Bay, FL. Remote Sensing of Environment 93: 423-441.

McKee, L., and Eyre, B. 2000. Nitrogen and phosphorus budgets for the sub-tropical Richmond River catchment, Australia. Biogeochemistry **50**, 207-239.

McKee, L.J., Ganju, N.K., and Schoellhamer, D.H., 2006. Estimates of suspended sediment entering San Francisco Bay from the Sacramento and San Joaquin Delta, San Francisco Bay, California. Journal of Hydrology 323: 335-352.

McClain, C.R., Feldman, G.C., Hooker, S.B., 2004. An overview of the SeaWiFS project and strategies for producing a climate research quality global ocean bio-optical time series. Deep-Sea Research II 51: 5-42.

Miller, R.L., McKee, B.A., 2004. Using MODIS Terra 250 m imagery to map concentrations of total suspended matter in coastal waters. Remote Sensing of Environment 93: 259-266.

Nixon, S.W. et al., 1996. The fate of nitrogen and phosphorus at the land-sea margin of the north Atlantic Ocean. Biogeochemistry 35, 141-180.

Robson, B.J., Bukaveckas, P.A., and Hamilton, D.P., 2008. Modeling and mass balane assessments of nutrient retention in a seasonally-flowing estuary (Swan River Estuary, Western Australia). Estuarine, Coastal and Shelf Science 76, 282-292.

Ruhl, C.A., Schoelhammer, D.H., Stumpf, R.P., and Lindsay, C.L., 2001. Combined use of remote sensing and continuous monitoring to analyze the variability of suspended-sediment concentrations in San Francisco Bay, California. Estuarine, Coastal, and Shelf Science 53: 801-812.

Schoellhamer, D.H., 2009. Suspended sediment in the Bay: Past a tipping point. Published in The Pulse of the Estuary: Monitoring and Managing Water Quality in the San Francisco Estuary. SFEI Contribution #583. San Francisco Estuary Institute. Oakland, Ca.

Shi, W., Wang, M., 2007. Detection of turbid waters and absorbing aerosols for the MODIS ocean color data processing. Remote Sensing of Environment 110: 149-161.

Sipelgas, L., Raudsepp, U., Kouts, T., 2006. Operational monitoring of suspended matter distribution using MODIS images and numerical modeling. Advances in Space Research 38: 2182-2188.

Wang, M., 2007. Remote sensing of the ocean contributions from ultraviolet to near-infrared using the shortwave infrared bands: simulations. Applied Optics 46: 1535-1547.

Wang, M., Shi, W., 2005. Estimation of ocean contribution at the MODIS near-infrared wavelengths along the east coast of the U.S.: Two case studies. Geophysical Research Letters 32: L13606.

Wang, M., Shi, W., 2007. The NIR-SWIR combined atmospheric correction approach for MODIS ocean color data processing. Optics Express 15: 15722-15733.

Wang, M., Tang, J., Shi, W., 2007. MODIS-derived ocean color products along the China east coastal region. Geophysical Research Letters 34: L06611.